



Physico-mechanical and Tribological Characteristics of Flax–Ramie Fiber Reinforced Green Composites and Anticipation of Fabricated Composites Under Different Loading with Sliding Constraint

Santosh Kumar¹ · Vijay Kumar Mahakur¹ · Sumit Bhowmik¹

Received: 3 June 2023 / Accepted: 21 August 2023 / Published online: 13 September 2023
© King Fahd University of Petroleum & Minerals 2023

Abstract

The plant-based cellulosic fibers have established much devotion in engineering research areas to reduce greenhouse depletion and improve environmental sustainability. Thus, the aim of this study is to develop green composites from flax–ramie reinforced with bio-epoxy matrix using hand compression molding. The fibers are reinforced unidirectional at 10%, 20%, 30%, and 40% weight fraction and characterized the structural, physical, and tribological behaviour of developed composites. The structural integrity and thermal stability have been analyzed using degree of crystallinity and thermogravimetric behaviour of composites. The pin on disc tribology test has been conducted based on different input parameters such as fiber weight fraction, composite types (flax composite, ramie composite, and hybrid composites), applied load (25 N, 50 N), sliding speeds (1 m/s, 2 m/s, and 3 m/s), and sliding distance (1000 m, 2000 m, and 3000 m). The results revealed that the inclusion of flax fibers with bio-epoxy matrix sustained greater thermal stability with wear and friction resistance compared to ramie fibers. Overall, the composite with 30% fiber loading provided greater crystallinity, stability, and finest tribology performance with minimal void formation among other developed composites. The microscopy analysis confirmed about the greater microstructural adhesion between fiber and matrix. The failure of composites at worn surface has been analyzed in terms of matrix cracking, fiber scattering and deformation due to higher loading and sliding distance. Finally, the influence of input constraints on tribological performances like wear loss, friction force, frictional co-efficient, and interface temperature have been predicated using artificial neural network.

Keywords Green composite · Structural composition · Thermal stability · Physical properties · Tribology · Artificial neural network

1 Introduction

In recent years, several worldwide corporations have focused on new fields such as power, construction, and transportation to generate their products using green engineering approaches [1]. Additionally, previous survey research on marketing tactics has shown that eco-friendly commodities are expected to grow significantly in the coming decade. Various firms have recently focused on breakthrough material discoveries that will be lighter without compromising particular strength. Furthermore, these unique compounds

should have better power efficacy and lifespan that, promotes greater abrasive durability. Considering these issues, manufacturing sectors concentrate substantially on developing sustainable composites using fiber/filler reinforcement that can affordably achieve the ultimate component [2, 3]. Synthetic-based polymer materials have been employed for a multitude of purposes, including load-bearing engineering materials [4–6]. Also, the lifespan of worn parts may lead to more cost-effective operation by requiring less maintenance. Nevertheless, restrictions such as non-biodegradable features resulted in an assessment of ecological problems which produces higher carbon foot-print to the environmental and became a serious obstacle to subsequent product development.

As a consequence, advancements in greener tribology in the perspective of adopting biodegradable components into tribological investigation can meet a wide variety of

✉ Sumit Bhowmik
bhowmiksumit04@yahoo.co.in

¹ Department of Mechanical Engineering, National Institute of Technology Silchar, Silchar, Assam 788010, India



requirements while also offering environmental benefits. Material researchers are in charge of creating an optimum design by building an appropriate eco-material framework with long-term properties for tribological applications. Several research investigations have taken place to assess the potential usage of biodegradable components based on natural fibers as a feasible substitute for conventional types [7–9]. When exposed to environmental conditions, these natural fiber materials exhibit characteristics of benign repercussions.

Natural fibers are significant in industries because of their increasing prevalence and unique properties. Additionally, due to their ecological advantages and exceptional specific mechanical performance, they are utilized in the construction, medical, marine and consumer domains to offer a wide range of beneficial goods [10–12]. The natural derived bio-based thermoset resin has got more potential to develop biodegradable and biocompatible green composite with natural fiber [13, 14]. The development of green composites only provided greater environmental sustainability but also produced higher specific strength, stiffness with cost effective and lighter weight materials for load bearing structural interior design in automotive, aerospace, and biomedical applications [15–17]. However, these cellulosic fibers have hydrophilic nature that has some complications like higher moisture capabilities, improper bonding, and instability during fabrication that reduced the overall performances and limited their applicability. Although, these limitations can be modified by chemical modification or treatment of fibers with different chemical process and improved their interfacial interaction and stability [13, 18]. The hybridization of fibers with different fibers is the other effective process to overcome these limitations and improved their usages capabilities for various structural application [19–21].

Among numerous natural fibers, flax and ramie fibers are found as the principal reinforcement with the polymer resin because of their exceptional mechanical qualities in terms of flexibility and stiffness, respectively. Moreover, their good strength, ease of availability and ease of fabrication encourage them highly appealing for polymer-based components [22–24]. These fibers are now employed in variety of industrial areas, notably in textiles and load-bearing conditions. As a result, it is important to look into and examine the tribological behaviour of innovative composites in hopes of broadening potential application to variety of production industries [25].

Till far, very few studies have focused on the tribological characteristics of flax-based and ramie-based matrix composites. Fu et al. first proposed that incorporating flax fiber into resin gave higher stability and resistance to wear during tribological testing [26]. Singh et al. also assessed the tribological testing and claimed that the hybrid composite

containing flax, hemp and 30° oriented carbon fiber exhibited better wear and erosion resistance [27]. Kamaraj et al. optimized the wear performance of the flax-based composite where graphene was incorporated. And the best wear resistance performance was seen at the lowest sliding speed and load, as well as at the highest sliding velocity [28]. Singh et al. applied MADM approaches to enhance the tribological performance of several natural fiber-based composites and discovered that ramie fibre composites had the greatest wear resistance performance [29].

The fundamental method for conveying tribological interactions is generally inadequate and unhelpful for acquiring a complete understanding. As a result, the evolution of artificial neural network (ANN) algorithms has been devised to visualise a sophisticated tribological challenge. The assessment of an ANN, in which neurons interchange all data, is prompted by the human neuron system. This technique employs three distinct stages input, hidden and output to construct computational equations. The communication among all stages is composed of neurons that are affected by extrinsic variables (weight and bias). The efficacy of ANN is determined by accumulating the weight with the input parameters, which is calibrated again by passing it into the concealed covers and then producing the relevant information in the form of outcomes [30–32].

The various studies were conducted to examine the thermo-mechanical properties of flax and ramie fiber composites; but limited work were reported on the tribological behaviour of these fiber reinforced composites. Moreover, the effects hybridization on physical, mechanical, thermal, and tribological behaviour of flax and ramie fibers reinforced composites have not been done yet. Therefore, this study deal to investigate the physical, mechanical, structural and tribological behaviour of flax–ramie-based reinforced composite. The hybridization effects of flax and ramie fiber at different weight fraction on their performances have been also characterized. Further, the influence of numerous parameters like load, speed, and sliding distance on the wear-resistant attributes are considered. Ultimately, after accumulating wear-related values from the experiments, ANN models are developed by introducing three distinct networks to anticipate the hybrid composite's tribological performance.

2 Materials and Methods

The reinforcing and matrix materials are selected on the basis of their physical, chemical, mechanical, and thermal performances. The composites have been fabricated at different weight fraction of flax and ramie fiber with bio-epoxy matrix resin then, characterize the physical and tribological behaviour.

2.1 Material

The FormuLITE series bio-epoxy resin has been used as matrix materials that, purchased from Cardolite Pvt. Ltd. Mangalore, India. The bio resins are extracted from Cashew nutshell liquid natural phenolic resources. It is having 44% bio-content with lower viscosity (905cPs) and lower density (1.08 g/cm^3) that cured at room temperature and provided greater wetting and stabilities [17, 33]. Two different continuous bast fibers (flax and ramie fibers) have been used as reinforcing materials to developed green composites. The flax and ramie fibers are derived from outer layer of stem of natural flax and ramie plants. These fibers are purchased from Go-green Products, Alwarthirunagar, Chennai-87, India and their basic physical and chemical parameters have been listed in Table 1. The potential of these flax and ramie fibers has provided greater strength, stability, suitability, disability, and compatibility compared to other natural fibers that can be a favorable material to replace conventional and synthetic materials [34, 35].

2.2 Fabrication Method

The compression mould technique has been used to fabricate flax–ramie reinforced bio-epoxy green composites. The fabrication process of green composites has been illustrated in Fig. 1. Two moulds (lower and upper) made with cast iron having dimension of $200 \times 200 \text{ mm}$ are used for fabrication process. Now, the mixture of FormuLITE 2501A resin and hardener 2401B are mixed properly in the ratio of 10:3 using mechanical stirrer and the process of degassing is done for 15–20 min to detect the air bubbles and air trap from the mixture. The continuous flax and ramie fibers are

orientated unidirectional on lower mould and the prepared mixture of resin and hardener are spread over the fibers. The roller has been used for proper distribution of matrix materials inside fibers and stacked properly. Based on the previous studies, the flax (F) and ramie (R) fibers have been reinforced at 10%, 20%, 30%, and 40% weight fractions with bioepoxy (E) matrix. The hybridization of flax and ramie fibers at weight fractions of 5F% + 5R%, 10F% + 10R%, 15F% + 15R%, 20F% + 20R% have been also reinforced to develop different types of green composites. Now, compressed the fabricated plates with upper mould by using H8 nuts and bolts that provided uniform pressure throughout the samples. The final fabricated plates have been prepared with an average thickness of 6–8 mm. The fabricated plates are pre cured at room temperature within 12 h then, the fabricated plates are removed from mould and again cured at 50–60 °C for 3 h called post curing process. Finally, the plates are cut as per American Society for Testing and Materials (ASTM) standards using table saw cutting machine tribology tests.

2.3 Material Characterizations

The analysis of crystalline and their phase changes of response of fabricated green composites have been analyzed using X-ray diffractometer (XRD). The analysis has been performed on Panalytical X'Pert³ model XRD machine to measure intensity of the crystal structure with respect to scattering angle (2θ) from 0° to 50°. The test has been operated at 30 kV/15 mA with speed of 2°/min and step size of 0.05 under monochromatic radiation ($\text{CuK}\alpha$) with emitted wavelength of 0.154 nm [37]. The thermogravimetric analysis (TGA) of fabricated green composites has been carried out to analyze the degradation behaviour and thermal stability. The percentages weight loss under the influence of temperature of composites have been examined to analyse their degradation behaviour. The test has been performed under nitrogen gas atmosphere at heating rate of 10 °C/min with flow rate of 200 ml/min using Netzsch STA 449F3 model [36].

The physical characterization such as density, porosity, and surface hardness of developed green composites have been determined. The density of any composite materials specified their specific properties that proven to be the essential characteristics for required performances. Initially, the rule of mixture equation (i) has been used to identify the theoretical density of developed green composites. The experimental density of green composites has been examined using Archimedes principle of immersion technique has been implemented using Eq. (ii). The test conducted at ambient temperature and normal water has been used as medium of immersion with density of (0.9977 g/cm^3) as per ASTM D-792-98 standards [38]. Void contents (porosity) of developed green composites have been measured using equation of difference between theoretical and experimental density (iii) as

Table 1 Basic physical and chemical parameters of flax and ramie fiber [24, 36]

Parameters	Units	Flax fiber	Ramie fiber
Fiber diameter	microns	25–50	25–45
Thickness	gsm	172–176	165–175
Orientation	degree	0/90	0/90
Micro fibriller angle	degree	5–12	8–14
Density	g/cm^3	1.38–1.55	1.34–1.45
Cellulose	wt%	65–75	70–82
Lignin	wt%	2.0–3.2	1.5–5.9
Hemi-cellulose	wt%	18–24	10–15
Crystallinity index	%	65–70	60–65
Tensile strength	GPa	0.3–1.5	0.25–1.25
Young's modulus	GPa	20–40	15–30
Elongation at break	%	1.0–8.0	0.5–5.5



Fig. 1 Fabrication process of flax–ramie reinforced bioepoxy green composites

per ASTM D-273-70 standards [39]. The hardness of composite materials measured the resistance to penetration. The D-shore hardness tester has been implemented where, needle strength resists and penetrates on the developed green composite samples to measure surface hardness in terms of hardness number. The test has been performed at room temperature as per ASTM D-785-8 standards having dimension of 6.5 ± 0.5 mm thick on three samples for each green composites and reported the average values [40].

$$\text{Theoretical density } (\rho_{\text{theo}}) = (\rho_m \times V_m) + (\rho_f \times V_f) \quad (\text{i})$$

$$\text{Experimental density } (\rho_{\text{exp}}) = \frac{(W_i)}{(W_i) - (W_f)} \times (\rho_l - \rho_a) + \rho_a \quad (\text{ii})$$

$$\text{Void content } (\%) = \frac{\rho_{\text{theo}} - \rho_{\text{exp}}}{\rho_{\text{theo}}} \times 100 \quad (\text{iii})$$

where ρ_f and ρ_m = density of fiber and matrix respectively, V_f and V_m = volume fraction of fiber and matrix respectively, W_i = composite initial weight before immersion, W_f = composite final weight after immersion, ρ_l = Water density, and ρ_a = air density.

2.4 Tribology Test Setup

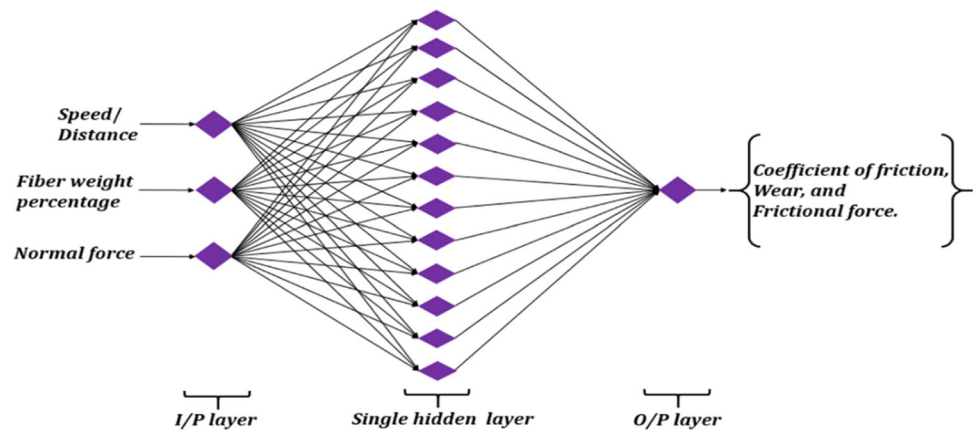
The pin of disc tribo-meter has been used to perform the tribology test and determine the friction and wear performance

of prepared green composites. The test has been performed dry conditions as well as at different environmental conditions on three samples for each composite with dimension of 15×10 mm as per ASTM G99-17 standard and reported the average values [41]. The developed samples have been fixed to the holder pin with 40 mm track diameter that slid on the counter disc. The counter disc has made of EN-31 harden steel having surface hardness and roughness of 68HRC and $0.6 \mu\text{m}$ respectively. The input parameter to conduct the test has been selected after different trial and methods. Finally, the test has been conducted by varying the sliding speeds of 1 m/s, 2 m/s, and 3 m/s at applied load of 25 N and 50 N. Furthermore, friction and wear performance of green composites have been also analyzed by varying the sliding distance up to 3000 m respectively.

2.5 Artificial Neural Network (ANN) Modelling

The incorporation of an ANN technique to generate comprehensive performance estimate datasets based on the connection of all examined factors has grown in popularity. ANN is used as a predictive model which belong to the class of Artificial Intelligence that creates statistical factors for any area due to their ability to predict the nonlinear features of wear variables, learning capacity, and growth of precise anticipation [42]. ANN is computationally cheap and can handle prediction adequately in case of less data also. The

Fig. 2 Schematic representation of artificial neural network anticipation model



MATLAB is used for this function because the ANN modelling method involves three fundamental stages, comprising training, testing, and validation to evaluate and estimate the essential behaviour for the specific kind of component [43].

In order to forecast the output factors such as wear, frictional forces, and coefficient of friction, three distinct nodes such as fiber weight percentage, load along with sliding speed and sliding length respectively, with one hidden layer are examined. Figure 2 represented the ANN anticipation model. The output is created concurrently throughout the modelling method. Training is confirmed using accessible experimental findings before being transferred to the concealed covers for the values to be augmented by diminishing mistakes detected over numerous repetitions. During the integration of the ANN model, 72 tested values are sorted into three groups. Among that, 70% of the tested data is used for training, while the remaining data is divided evenly and preserved for testing and validation. Throughout the ANN process, variables like the networks, transfer function and neurons are considered and these variables are altered numerous times in order to obtain the optimum ANN architecture for projecting the efficiency of constructed composites [44].

2.6 Surface Morphology

The worn surface structure and morphology of developed green composites have been analyzed using Quanta-200 scanning electron microscopy (SEM). Before analysis, the samples are coated with gold coating that helps in better transmission of electron through non-conductive polymeric composite samples. The has been carried out at passing velocity of 15 kV under magnification between $50 \times$ to $5000 \times$ at high vacuum conditions. The SEM analysis analyzed the wear texture, microstructure, and failure behaviour of developed green composites under loading constraints.

3 Results and Discussion

3.1 Structural Composition and Thermal Stability

The XRD analysis assessed the diffractograms and degrees of crystallinity of fabricated composites and illustrated in Fig. 3a. The intensity of diffraction bands has been examined and analyzed the amorphous and crystal phase areas with crystal sizes. The results showed that flax fiber composites (FRC) recorded greater intensity of Cellulose-I at distinct peaks $2\theta = 10^\circ$ and 13° with reflection of 101 crystallographic plane. The sharp 2θ peaks 18° corresponds to 002 reflections related with orthorhombic crystal structure of matrix. The ramie fiber composite (RRC) followed the trend with lower intensity of cellulose with reflection peaks $2\theta = 9^\circ$ and 12° at 101 plane and 16° for 002 crystal plane due to decrease in hydrogen bond network. These trends are analyzed in terms of changes in the macromolecular structure of biopolymer matrix with separation of intermolecular bond during mercerization and crunching [45]. The natural fibers present greater cellulose contents biomass that leads to higher monocrystalline fractions with greater proportion of amorphous [46]. Thus, chemical modification and hybridization have been done to enhance their hydrogen bond and declined the fibrillation amorphous structure. The hybrid composite showed greater intensity with sharp diffracting peaks due to increase of crystalline transition structure. The reflections peaks (2θ) are shifted to 14° and 17° correspond to 101 crystal plane and 25° for 002 crystallographic plane.

The thermal stabilities and degradation behaviour of fabricated composite have been analyzed under temperature ranges from room temperature to 600°C and showed in Fig. 3b. The results observed that the addition of fibers with polymer matrix provided greater stabilities up to 100°C with minimum loss of weight percentages (2–3%). The, the degradation of composites in between 100 and 250°C are analyzed due to desorption of gasses and loss of moisture. The major degradation has been analyzed from 250°C

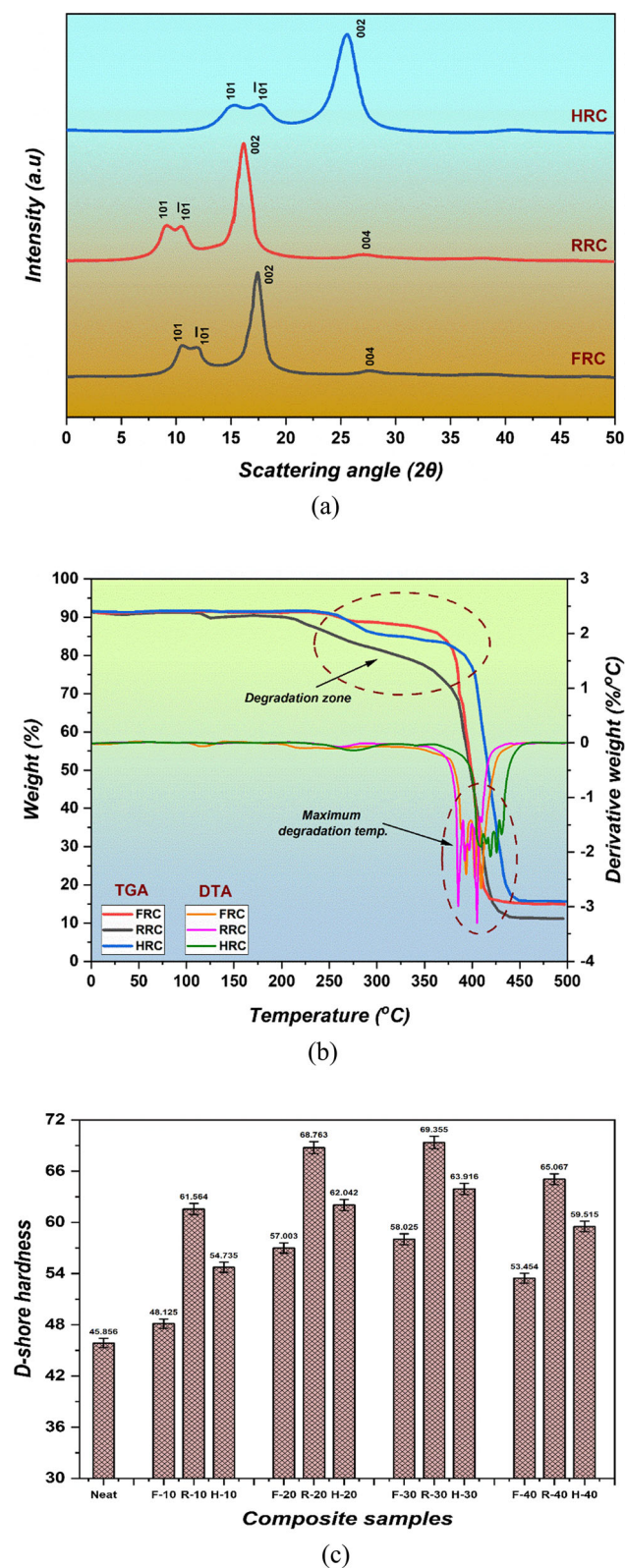


Fig. 3 **a** XRD analysis with their reflection plane of fabricated green composites. **b** Thermal stabilities and degradation behaviour of fabricated green composites. **c** D-shore surface hardness of fabricated green composites

to 430 °C due to decompositions of cellulose, hemicellulose, lignin, and wax. Beyond 420 °C, the thermal stabilities affected and drastically reduced the mass loss due to condensation and reorganization process of carbonize materials [47, 48]. Finally, the generated residue from carbonization stages are inorganic dust that showed a constant weight in the final stage. Table 2 tabulated the degradation temperature in every stages for all composites. The hybridization of fibers enhanced the degradation behaviour due to greater interfacial bond with dual fiber nature and followed FRC and RRC. The FRC composites showed greater thermal stabilities with higher degradation temperature due to higher lignocellulose contents of flax fibers. Moreover, the flax fibers also have higher micro-fibriller angle that sustained extra oxidative decomposition compared to ramie fibers [36].

3.2 Physical Properties Results

The density and porosity of developed green composites have been examined and tabulated in Table 3. The results analyzed that, the inclusion of fibers with bio-epoxy matrix at different weight fraction have increased their overall theoretical density and observed maximum for flax composites with 40% weight fraction of fiber (F-40). This is because, density mainly depends on the reinforcement materials during rule of mixture where, the flax fiber (1.38 g/cm³) has higher density compared to ramie fiber (1.34 g/cm³). The experiment densities of developed composites have also been recorded higher for flax fiber composites compared to ramie composites and hybrid composites because, flax fibers have greater cylindrical lumen diameter that absorbed higher % of water during immersion process [49].

The void formation (porosity) of developed composites has been calculated from difference between theoretical and experimental density [50]. The difference has been higher for ramie fiber composites, thus, void formations are greater for ramie fiber composites compared to flax fiber composites. The 30% reinforcement of fibers with matrix have recorded lower void formation due to higher crosslink bond with greater compactness between fiber and matrix. The further increments of fiber loading (40%) increased the void formation due to improper bond and clusterization of fibers. The hybridization of fibers decreased the experimental density due to dual fiber interfacial bond that absorbed lower percentages of water compared to single cellulosic fibers [51, 52].

The surface hardness of developed green composites has been discussed and illustrated in Fig. 3c. The results measured the localized plastic deformation resistance in terms of hardness number. The inclusion of fibers up to 30% increased the hardness values due to increment of their elastic deformation and stiffness. This is happened due to higher interfacial interaction within epoxy matrix and fibers reinforcement that

Table 2 Degradation behavior and degradation temperature of fabricated green composites

Composites	Initial degradation (%)	Maximum degradation (%)	Maximum degradation temperature (°C)	Char residue (%)
FRC	3.75	72.69	403	15.23
RRC	6.24	76.45	384	11.06
HRC	4.03	71.36	418	17.77

Table 3 Developed green composites at different weight fraction with density and void content

Composite notation	Weight percentages (%)			Volume fraction of composites			Theoretical density (g/cm ³)	Experimental density (g/cm ³)	Void content (%)
	F*	R*	E*	F	R	E			
F-10	10	0	90	7.246	0	83.334	1.104	1.0695	3.125
R-10	0	10	90	0	7.463	83.334	1.101	1.0657	3.203
H-10	5	5	90	3.623	3.731	83.334	1.103	1.0689	3.092
F-20	20	0	80	14.493	0	74.074	1.129	1.0978	2.763
R-20	0	20	80	0	14.925	74.074	1.124	1.0922	2.832
H-20	10	10	80	7.246	7.463	74.074	1.126	1.0953	2.726
F-30	30	0	70	21.739	0	64.815	1.155	1.1247	2.623
R-30	0	30	70	0	22.388	64.815	1.147	1.1159	2.711
H-30	15	15	70	10.869	11.194	64.815	1.151	1.1212	2.579
F-40	40	0	60	28.985	0	55.556	1.183	1.1431	3.337
R-40	0	40	60	0	29.851	55.556	1.171	1.1259	3.385
H-40	20	20	60	14.493	14.925	55.556	1.177	1.1409	3.306

*F tends to flax fiber, R tends to ramie fiber, and E tends to bio-epoxy matrix

Table 4 Mechanical performance and glass transition temperature of flax–ramie fiber composites [24]

Composite notation	Tensile properties		Flexural properties		Compressive properties		Glass transition temp (<i>T_g</i>)
	Strength (MPa)	Modulus (GPa)	Strength (MPa)	Modulus (GPa)	Strength (MPa)	Modulus (GPa)	
F-10	72.03	3.09	114.24	6.51	76.34	3.80	83
R-10	77.91	2.91	98.43	6.90	73.33	3.55	85
H-10	75.87	4.16	102.12	7.28	83.63	4.94	88
F-20	79.95	3.98	130.91	9.39	102.35	5.69	89
R-20	91.43	3.42	109.30	9.92	94.92	5.19	91
H-20	85.73	5.02	119.72	10.22	110.32	7.33	98
F-30	87.82	4.38	144.25	11.17	120.95	6.75	92
R-30	108.39	3.85	119.08	11.68	112.03	6.29	95
H-30	102.24	5.63	138.31	12.53	130.0	8.87	110
F-40	66.56	3.12	104.66	6.27	72.21	3.72	76
R-40	71.33	2.97	86.24	6.36	64.45	3.39	79
H-40	69.55	4.01	93.59	6.95	76.78	4.54	82

sustained higher load without plastic deformations [53, 54]. The maximum hardness values have been recorded for R-30 composites (69.355) and followed by H-30 and F-30 composites (58.025 and 63.196) respectively. The results observed that, the ramie fiber composite analyzed higher hardness values compared to flax fiber composites because the ramie fibers are more hard than flax fiber that provided greater interface linking density and resist the plastic deformation [36]. Further increments of fiber loading after 30% i.e. F-40, R-40, and H-40 composites declined their strength stiffness, stabilities, impact and hardness performances due to debonding and clusterization formation that formed weaker bond between fibers and matrix [55].

3.3 Mechanical Performance of Composite

The mechanical properties and dynamic mechanical analysis of flax–ramie fiber composites have been already examined in the previous study and tabulated in Table 4 [24]. The results observed that the inclusion of fibers up to 30% with bio-epoxy matrix have enhanced their tensile, flexural and compressive properties with greater thermal stability and viscoelastic properties. The improvements have been observed due to higher interlocking bond with grater interfacial stress transfer between fibers and matrix. Figure 4 illustrated the fracture behaviour and adhesion behaviour of fiber with matrix for mechanical tested samples.

3.4 Tribological Characteristics

The tribology test of developed green composites has been conducted on dry condition at room temperature. The results have been analyzed in terms of wear loss (height loss), friction force and co-efficient of friction due to rubbing acting between samples and counter disc by varying the applied load (25 N and 50 N), rotation speeds, (1 m/s, 2 m/s, and 3 m/s) and sliding distance (1000 m, 2000 m, and 3000 m) respectively. The analyzed results have been discussed in three different sections by fixing one input and varying others.

3.4.1 Effects of Applied Load and Sliding (Rotation) Speed

The wear loss (WL), frictional force (FF), interface temperature (IT) and co-efficient of friction (CoF) of developed composites have been measured under influence of applied load (25 N and 50 N) and sliding velocities (1 m/s, 2 m/s, and 3 m/s) and illustrated in Fig. 5a, b, and c respectively. The results analyzed that at constant load of 25 N, the behaviour of WL, FF, and CoF are maximum for 10% of flax and ramie fibers loading (F-10, R-10, and H-10 composites) while, further addition of fibers up to 30% declined their respective tribological behaviour because natural fibers are cellulosic

in nature and has some moisture content inside lumen structure of fibers that reduced the penetration rate during rubbing on counter disc [56]. The 30% loading of fibers also provided greater interfacial interlocking bond with bio-epoxy matrix that sustained higher stress transfer load during tribology test and observed lower wear loss of composites (F-30, R-30, and H-30). Further addition of fibers (40% loading) suddenly increased the wear and frictional behaviour because higher loading of cellulosic fibers tends to agglomerate that reduces the interlocking bond between matrix and fibers due to debonding and clusterization effects [55, 57].

The increments in load from 25 to 50 N drastically increased the wear and friction values as shown in Fig. 5a and b due to high penetration and depth concentrated on the counter disc that increased the ploughing and wear debris on the samples [58, 59]. Moreover, the increments in rotational speeds from 1 to 3 m/s also increased the wear and frictional behaviour because higher rate of rotation increased the friction between samples and counter disc. The rate of increments in WL, FF, CoF, and IT at 50 N load are quite high for 10% and 40% of fiber loading compared to 20% and 30% fiber loading because 10% of fibers loading have higher percentages of polymeric matrix that get soften at higher load during rubbing due to generation of higher interface temperature. It reduced the interfacial bonding between fibers and matrix and generated higher wear debris [60, 61]. While, 40% fiber loading created debonding and agglomeration in developed green composites that increased the frictional thrust at higher load with high velocity and increased the overall wear and friction [62, 63].

The results also analyzed that, the ramie fiber composites recorded higher wear and tear behaviour compared to flax fibers because ramie fibers have higher brittleness with lower deformation and elastic behaviour [36]. The brittleness phenomena of thermoset matrix with fiber reinforced composites increased the frictional thrust at higher load and created extra cracks with more material removal and film formation during rubbing action on the counter disc and finally, fracture of composite samples have been analyzed [57, 64]. The hybridization of flax with ramie fibers have observed optimal wear and frictional behaviour compared to single fiber composites due to higher compactness and synergetic effects of dual fiber natural. The similar trends have been analyzed for all developed green composites but, the rate of increments in wear loss has been recorded maximum at 2 m/s sliding speeds (50–60% for all composites) while, CoF and IT are more stable as compared to WL and FF as shown in Fig. 5c. Further increment of sliding speeds (3 m/s) also increased the wear and frictional values but, the rate of increments has been reduced up to 25–30% for all composites.



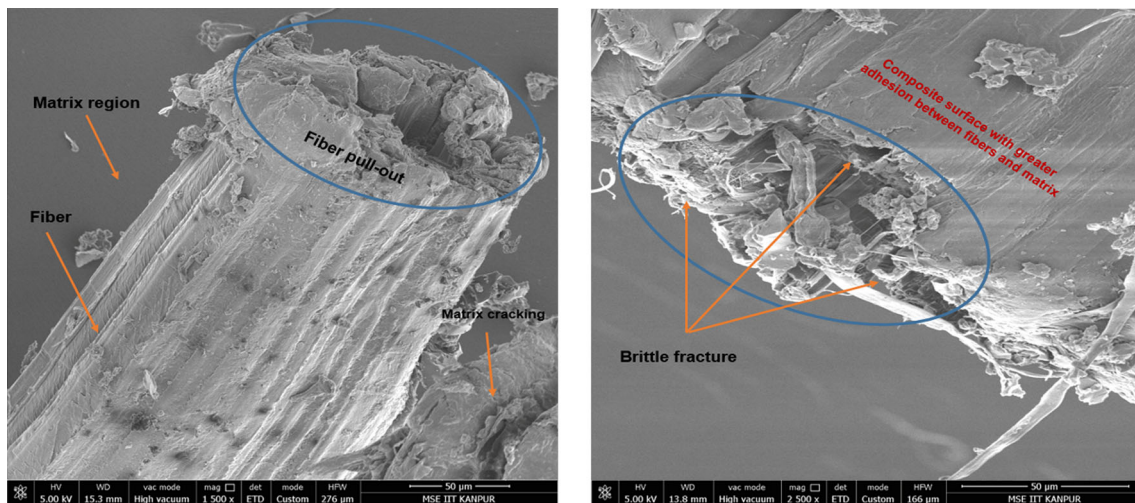


Fig. 4 Surface morphology and adhesion of developed green composites

3.4.2 Effects of Sliding Distance and Applied Load

The effects of variable sliding distances at 25 N and 50 N applied load have been analyzed for all developed composites. From Fig. 6a, the results exhibited that wear loss of composites have been increased with increase in sliding distance and furthermore, the values of wear loss drastically increased due to increment in applied load. The impact and penetration on counter disc are high at higher load that created greater grooves and increased the material removal rate [58, 65]. The co-efficient of friction (CoF) values for all developed composites have been illustrated in Fig. 6b and observed that the values are increased with increase in applied load. However, CoF values are independent on increase in sliding distance because CoF of composites depends on the penetration rate and friction generation on the counter disc. Thus, the greater penetration rate will be generated at higher load that increased the CoF values. While, with increase in sliding distance (more than 1500 m), the fibers thin film like debris, tear, and scars have been formed on counter disc that reduced the penetration rate due to reduce in friction [66, 67]. So, the CoF values have been decreased after certain sliding distance for all developed composites. The similar trends for frictional force (FF) and interface temperature (IT) have been observed hence are not displayed with figure.

Based on experimental observations, the ramie fiber composites observed little bit higher wear and frictional values due to more brittleness and lower elastic behaviour of ramie fibers compared to flax fiber. Overall, the 30% flax fiber composites (F-30) have analyzed lowest values of wear loss 43.69 μm at 25 N and 138.14 μm at 50 N applied load with minimum values of co-efficient of friction (0.348 and 0.527) in between 500 to 1000 m sliding distance respectively. The maximum WL (255.77 μm) and CoF (0.635) have been

observed for R-10 composites at 50 N load because matrix percentage are higher (90%) in these composites that get soften during rubbing at higher load and decreased the interfacial strength between fibers and matrix. Thus, excessive wear loss with greater wear and tear have been observed. The R-40 composites have also observed higher wear and tear because at higher loading of fiber (40%), agglomeration and clusterization of fibers have been analyzed that results poor adhesive bond with matrix. Therefore, the materials failed early due to debonding that created excessive materials removal and ploughing at higher load [57, 61]. The hybridization of flax fibers with ramie fiber showed greater interfacial strength compared to single flax/ramie fiber composites. Thus, the resistance in wear and frictional behaviour for hybrid composites have been analyzed.

3.4.3 Effects of Rotation Speed and Sliding Distance

The friction and wear performance of prepared green composites have also been analyzed under the influence of rotation speed (sliding velocity) at variable sliding distance. Figure 7a showed the wear loss of developed composites and analyzed that, the wear loss has been enhanced with increase in sliding speeds under variable sliding distance. The results showed linear behaviour of increment in wear loss under increase in sliding distance and sliding speed. However, the rate of increments in wear loss are higher at 3 mm/s compared to 1 m/s and 2 m/s because at higher speed, the sudden thrust will be generated at counter disc due to rubbing and created higher tear and scratch on the composites samples [59]. The composites with 10% and 40% of ramie fiber loading (R-10 and R-40) recorded maximum wear loss of 195.12 μm and 184.03 μm at 25 N load with sliding speed of 3 m/s and followed with 20% fiber and 30% fiber loading.

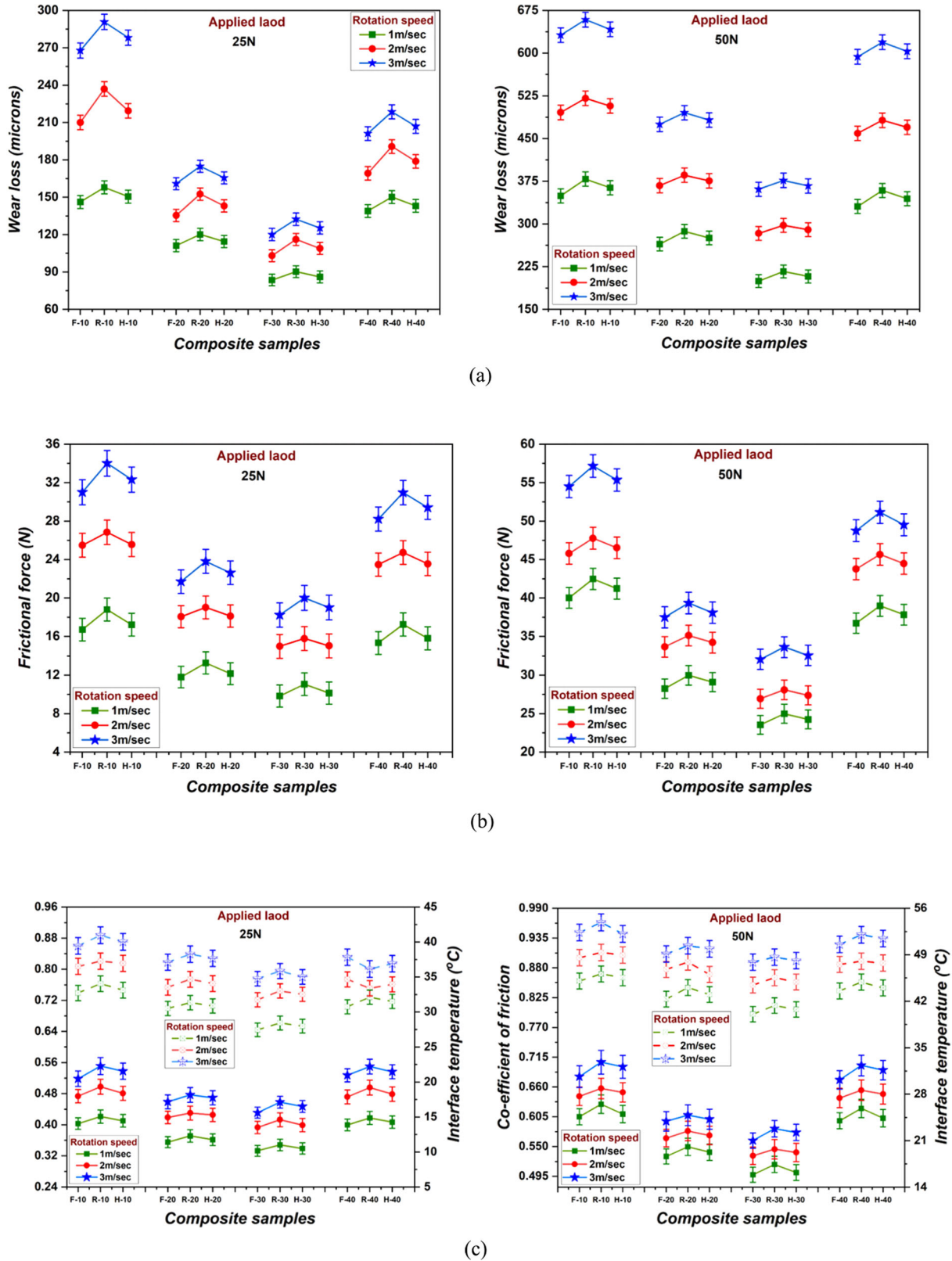
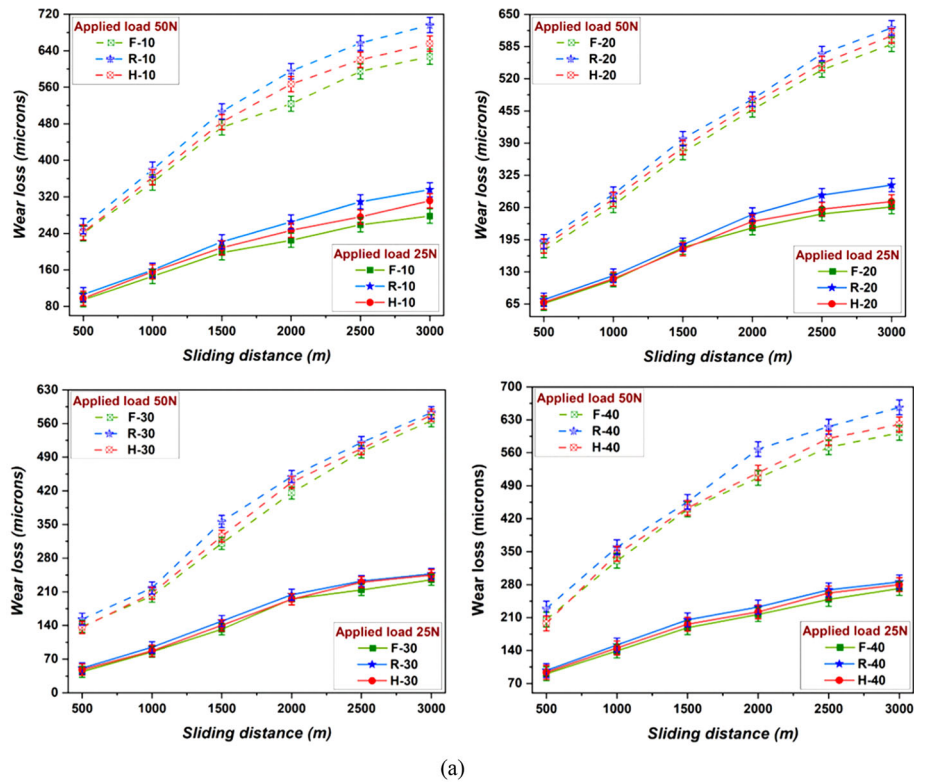


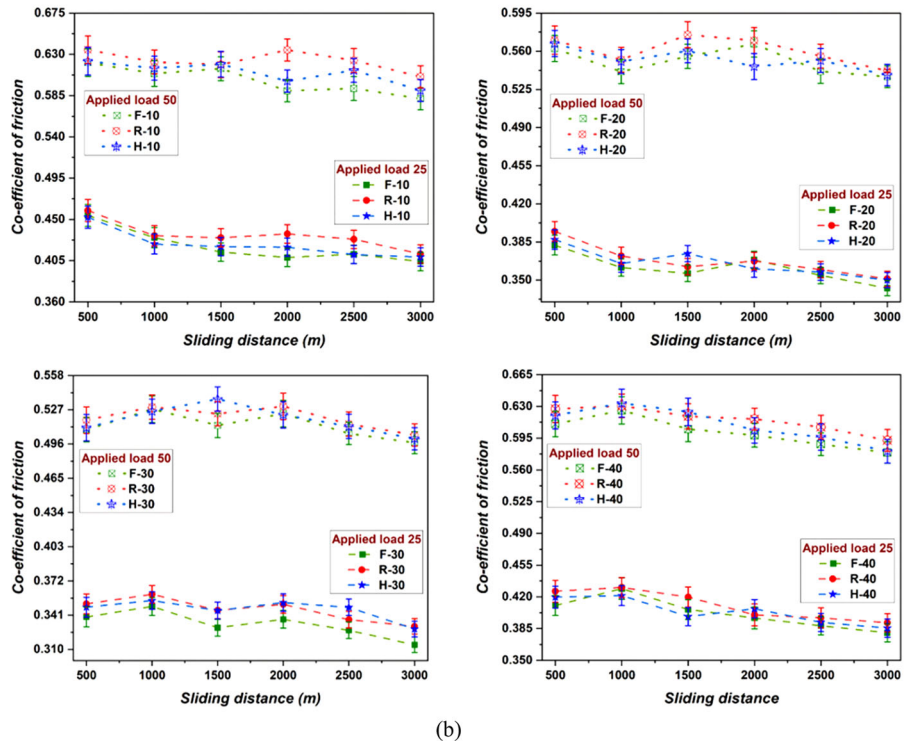
Fig. 5 a Wear loss of developed green composites at 1 m/s, 2 m/s, and 3 m/s sliding speeds under 25 N and 50 N applied load respectively. **b** Frictional force of developed green composites at 1 m/s, 2 m/s, and 3 m/s sliding speeds under 25 N and 50 N applied load respectively.

c Co-efficient of friction and interface temperature of developed green composites at 1 m/s, 2 m/s, and 3 m/s sliding speeds under 25 N and 50 N applied load respectively

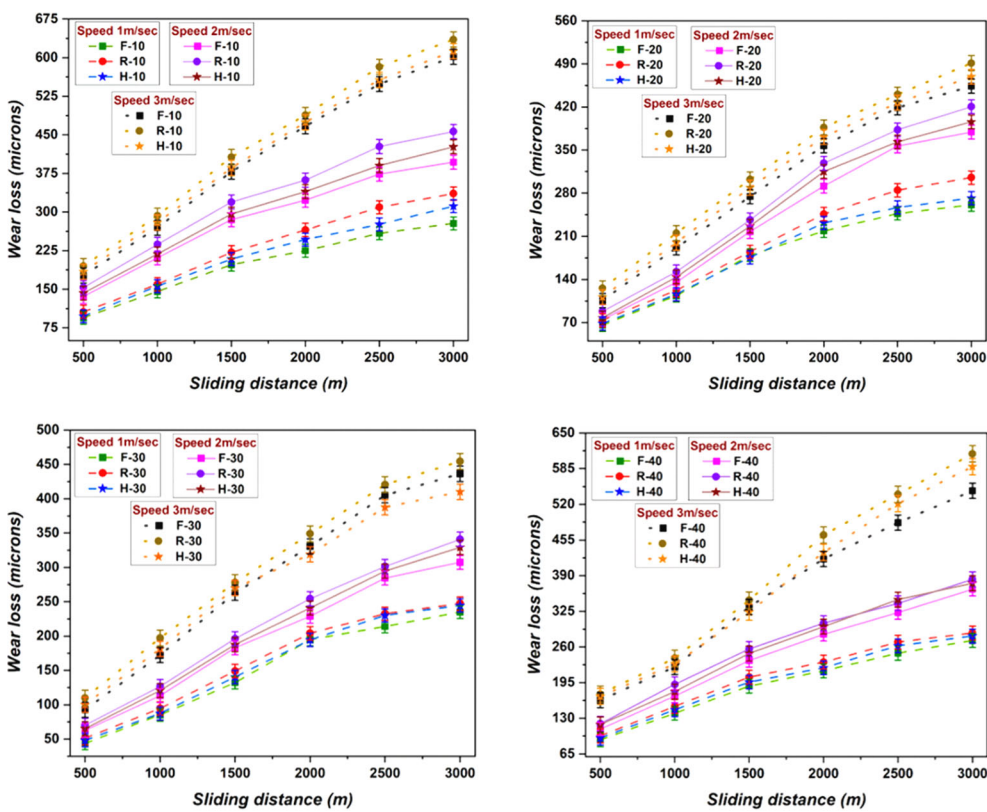
Fig. 6 a Wear loss of developed green composites at variable sliding distance under 25 N and 50 N applied load respectively. **b** Co-efficient of friction of developed green composites at variable sliding distance under 25 N and 50 N applied load respectively



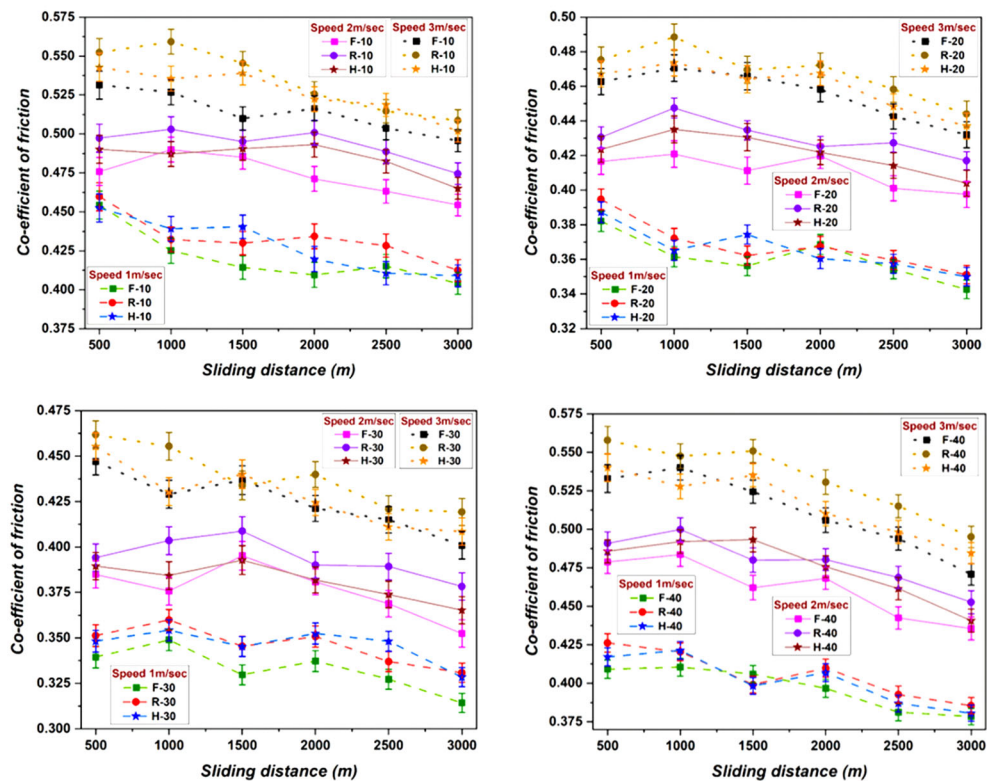
(a)



(b)



(a)



(b)

Fig. 7 a Wear loss of developed green composites at variable sliding distance under 1 m/s, 2 m/s, and 3 m/s sliding speeds respectively. b Co-efficient of friction of developed green composites at variable sliding distance under 1 m/s, 2 m/s, and 3 m/s sliding speeds respectively

The co-efficient of friction (CoF) values of all developed composites has been showed in Fig. 7b. The results noticed that, the CoF values are fluctuating under the influence of sliding distance. More the sliding speed more fluctuating in CoF values have been observed. It also analyzed that after certain sliding distance (500–1000 m), the CoF values are decreasing because after some sliding distance, the wear debris and scars are stacked at counter disc that reduced the penetration rate and friction between composite samples and counter disc [67]. The composite with 30% fiber loading analyzed the lowest values of CoF because natural cellulosic fibers are hydrophilic in nature that have some moisture inside cellular structure fibers [63]. During rubbing, the debris and scars of these natural fibers are acted as lubricating action and reduced the frictional co-efficient values. While further increment of fiber loading (40%) increased the CoF because, the developed composites have poor adhesion characteristics that formed more voids and cracks. At higher load and sliding speed, these cracks are propagated and created higher grooves during rubbing. Thus, higher grooves provided higher penetration rate with maximum wear and tear behaviour on composite samples [58, 66]. The CoF values are 0.559 at 25 N and 0.699 at 50 N for R-10 composites at 3 m/s then followed by H-40 (0.534, 0.689) and F-40 (0.527, 0.673) composites respectively.

3.5 Anticipation Through ANN Method

In order to evaluate the constructed ANN, the mean square error (MSE) is computed to quantify the trained values, which indicates the tribological characteristics of the developed material, and the expression for MSE is presented in Eq. (iv). This experimental values are iterated several times until the convergence conditions are met. The error is estimated by comparing the anticipated and actual readings [42]. The standard deviation (SD) and mean error percentage are also estimated, using the expressions stated in Eqs. (v) and (vi).

$$MSE = \sum_{I=1}^n (L - l)^2 \tag{iv}$$

$$\text{Mean error \%}, M = \left\{ \sum_{i=1}^n \left[\frac{(p - P) \times 100}{\text{Original}} \right] \right\} / N \tag{v}$$

$$SD = \left[\frac{\sum (M - m)^2}{N - 1} \right]^{1/2} \tag{vi}$$

where I is the iteration count and l and L are the anticipated and real validation outcomes, respectively. N is the experimental values count, whereas p and P denote the predicted

and real data, respectively. M denotes the mean error percentage, and m is the avg. mean error percentage of the real data.

The three different networks such as layer recurrent, cascade back, and feed forward back-propagation are employed for analyzing the ANN anticipation. Among numerous networks, the back-propagation network was recognized as the most efficient network for anticipation. To examine the network’s functioning, the numerous neurons and hidden layers must be altered. Yet, there are no specific guidelines for estimating the amount of neurons, networks, and hidden layers. As a result, the trial-and-error approach is utilized, and the network with the greatest outcome is chosen [58, 68]. Following the alteration of numerous variables during ANN modelling, the feed-forward back-propagation network with Purelin function and 11 and 10 neurons have provided the optimized outcome at constant sliding distance and speed respectively, for forecasting the developed materials as demonstrated in Tables 5 and 6.

As previously indicated, MSE acts as a computational framework to evaluate the efficacy of the ANN. Figure 8a depicts the MSE for all the designed networks. And in Fig. 8b, the MSE for network 5 is illustrated whose value is 0.11866, demonstrating that the revised ANN model provided an effective nonlinear performance to real obtained values.

As aforementioned, the Purelin function yielded the most significant results. As a consequence, MSE has been done solely with the Purelin function at various networks and neurons at a constant sliding speed parameter. Figure 9a depicts the MSE derived after accounting for the various factors for the results. The MSE for network 4 is 0.12786 illustrated in Fig. 9b, suggesting that the modified ANN model also provided effective nonlinear performance when compared to real-world values.

The regression graphs are represented to assess all the output variables (wear, frictional force and CoF). The identical scenario is depicted in Fig. 10a and b, with the flaws correlating to testing, training and validation methods. When the cluster draws nearer to the midline, the ANN model becomes more reliable. According to the study, the value for the correlation coefficient is 0.971 and 0.988, which is sufficient to reproduce the ANN model. The assessment of the ANN algorithm employing the Purelin function showed to be the most useful mechanism for estimating the tribological characteristics of varied fiber weight-based composites [43, 68].

3.6 Morphology Analysis at Worn Surface

The scanning electron microscopy (SEM) analysis has been done to identify the failure behaviour on worn surface during tribology test. The morphology of microstructure with adhesive behaviour between fibers and matrix have been also revealed. Figure 11a–f illustrated the morphological analysis

Table 5 Anticipation of ANN model at constant sliding distance considering Levenberg–Marquardt training function

Network count	Network types	No. of neurons	Wear		Frictional force		CoF	
			Avg. error%	SD	Avg. error%	SD	Avg. error%	SD
1	FFBP	7	9.5843	2.1594	- 7.9245	1.6613	- 2.5939	0.4981
2	FFBP	8	4.4591	1.011	- 4.9347	3.063	27.77	4.075
3	FFBP	9	5.7101	0.8365	0.5788	0.2832	- 0.6586	0.5533
4	FFBP	10	- 4.5998	1.0293	4.3221	0.9176	0.6286	0.1116
5	FFBP	11	1.893	0.291	3.3037	0.106	3.598	0.3189
6	FFBP	12	3.5198	0.4249	9.5334	1.9583	- 9.7483	2.2493
7	CFBP	7	9.6504	0.7265	7.2206	0.1963	2.0926	0.9228
8	CFBP	8	38.545	7.69	- 3.5591	1.498	- 25.0698	6.192
9	CFBP	9	7.7042	0.2999	8.7224	0.5221	2.5631	0.822
10	CFBP	10	- 6.5697	3.7604	5.5239	9.7895	- 16.966	6.0291
11	CFBP	11	10.6745	0.1071	19.6348	2.0624	0.2412	2.1696
12	CFBP	12	- 7.2541	0.6813	- 3.8981	1.4136	- 19.9758	2.0948
13	LR	7	203.788	22.693	77.166	4.938	18.433	17.754
14	LR	8	20.171	0.2878	20.652	0.1827	23.646	0.4706
15	LR	9	- 1.1707	2.2471	4.2164	1.0715	24.3342	3.3186
16	LR	10	5.9745	2.383	8.5375	2.9423	- 29.3494	5.3253
17	LR	11	6.2164	0.364	5.4829	0.2039	1.9461	0.5679
18	LR	12	19.4631	1.8606	8.4629	0.5398	4.8841	1.3208

Table 6 Anticipation of ANN model at constant sliding speed considering Levenberg–Marquardt training function

Network count	Network types	No. of neurons	Wear		CoF	
			Avg. error%	SD	Avg. error%	SD
1	FFBP	7	- 10.6965	0.8656	- 7.8622	0.2471
2	FFBP	8	- 38.9412	13.8698	23.6028	0.2216
3	FFBP	9	1.1683	6.5661	14.9314	10.1298
4	FFBP	10	2.2316	0.1463	0.9348	0.4293
5	FFBP	11	- 4.9515	0.5484	- 1.0777	0.297
6	FFBP	12	- 2.1534	0.2719	- 0.4899	0.0911
7	CFBP	7	7.8261	5.2651	95.1363	13.7875
8	CFBP	8	5.8055	0.8617	2.7643	0.198
9	CFBP	9	- 7.0616	0.8172	- 0.6086	0.5909
10	CFBP	10	33.0935	6.8937	- 9.84	2.4752
11	CFBP	11	17.151	2.2832	62.2889	7.5667
12	CFBP	12	14.9884	2.6343	- 4.952	1.7171
13	LR	7	- 0.8856	1.1183	- 22.1955	5.7685
14	LR	8	8.8797	0.3271	24.4299	3.0663
15	LR	9	0.4167	1.8049	- 9.2008	3.9036
16	LR	10	- 5.0776	0.5746	- 1.2756	0.2551
17	LR	11	- 8.2168	0.962	- 2.0131	0.3918
18	LR	12	- 3.4719	1.1709	- 1.5613	0.754

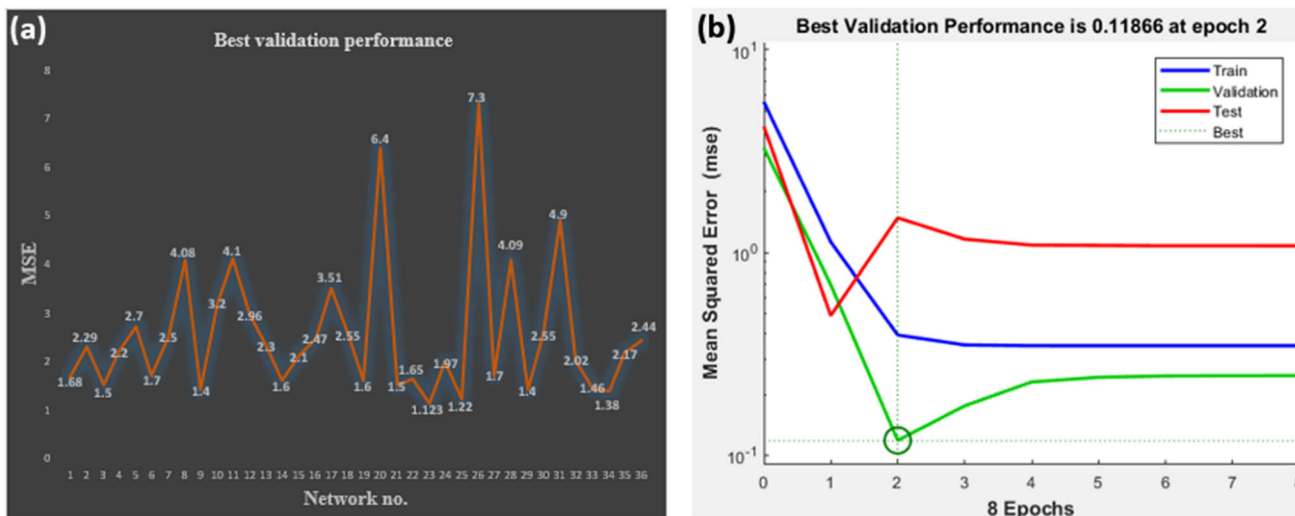


Fig. 8 a Representation of mean square error and b performance graph of the anticipated model for the data at constant sliding distance

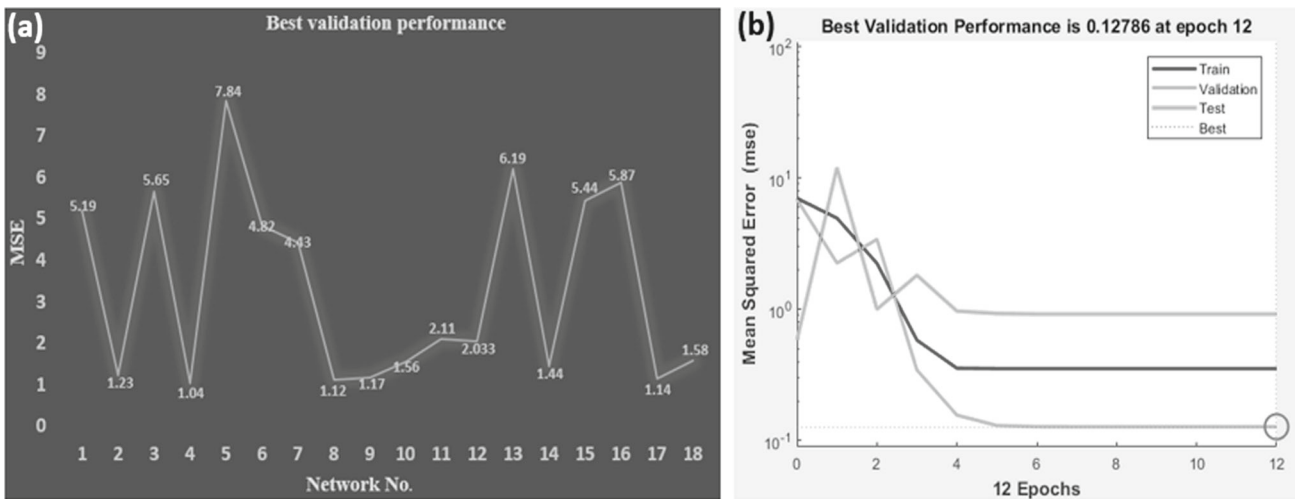


Fig. 9 a Representation of mean square error and b performance graph of the anticipated model for the data at constant sliding speed

of worn surface at 25 N and 50 N applied load, 1 m/s, 2 m/s, and 3 m/s sliding speeds with variable sliding distance. The wear and tear mechanism of developed green composites have been analyzed in form of fiber debris, scar and film formation, matrix cracking, plastic deformation, fiber scattering and delamination, tearing and pull-out of fibers, matrix-fiber breakage, grooves formation, crack propagation, high deformation, brittle fracture, and debonding between fiber and matrix due to high penetration rate and friction during rubbing on counter disc [62, 69].

Figure 11a showed greater adhesion between fiber and matrix of flax fiber composites where, the formation of films, debris, and scars have been analyzed at worn surfaces due to materials removal during rubbing. The cracks have been also formed due to increase in sliding distance and applied load. The ramie fiber composites showed higher brittleness

and compactness as displayed in Fig. 11b. Thus, nature of failure has been analyzed in form of higher wear and tear, matrix deformation, brittle fracture, and interfacial debonding at higher applied load under variable sliding distance. The 30% fiber loading composites showed greater interfacial adhesion that sustained high load. Therefore, Fig. 11c showed only fine grooves and cracks with formation of thin wear films, scars, and debris at worn surfaces. The higher loading of fibers (40%) agglomerated with bioepoxy matrix and failed early during rubbing with counter disc due to extra materials removal as shown in Fig. 11d. At higher loading and sliding distance, the fibers are scattered and teared due to clusterization and interfacial debonding. Therefore, the formation of material removal and wear debris are quite high compared to other composites. Due to higher brittleness nature of bioepoxy, matrix cracking has been

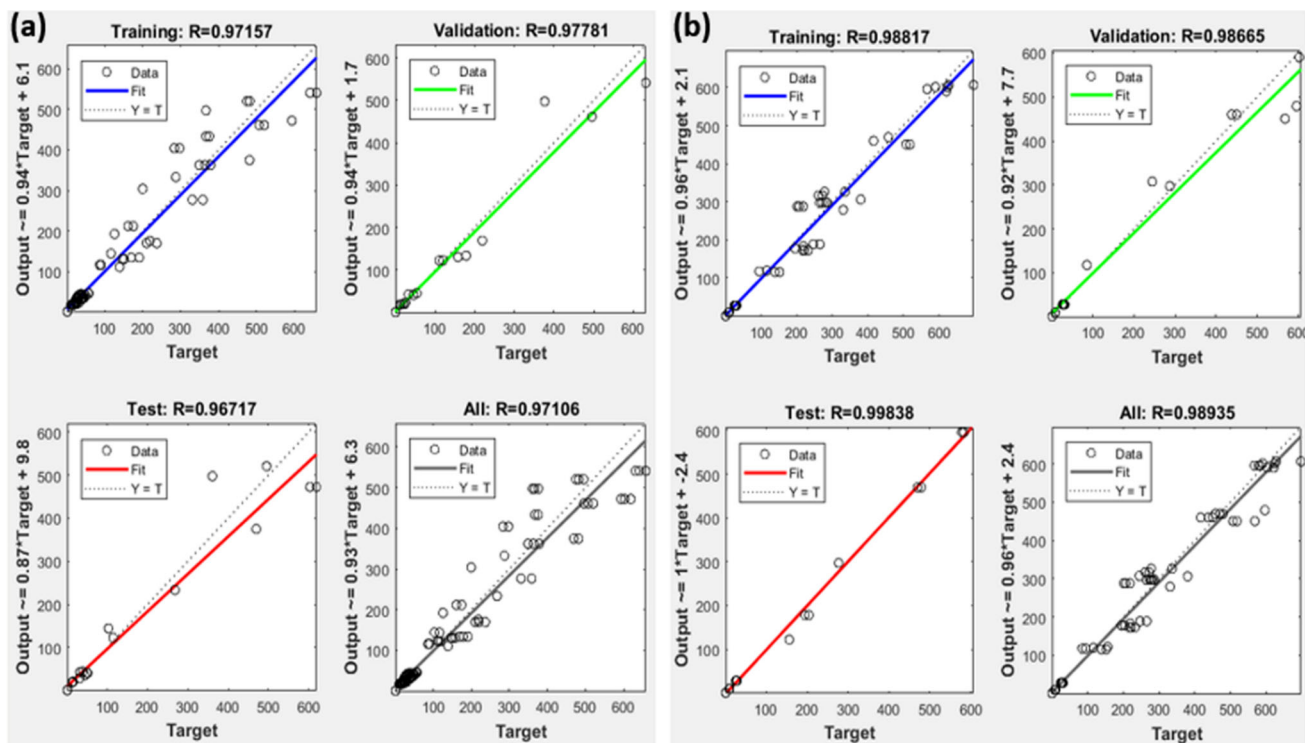


Fig. 10 Regression graph for anticipated model **a** at constant sliding distance, and **b** at constant sliding speed

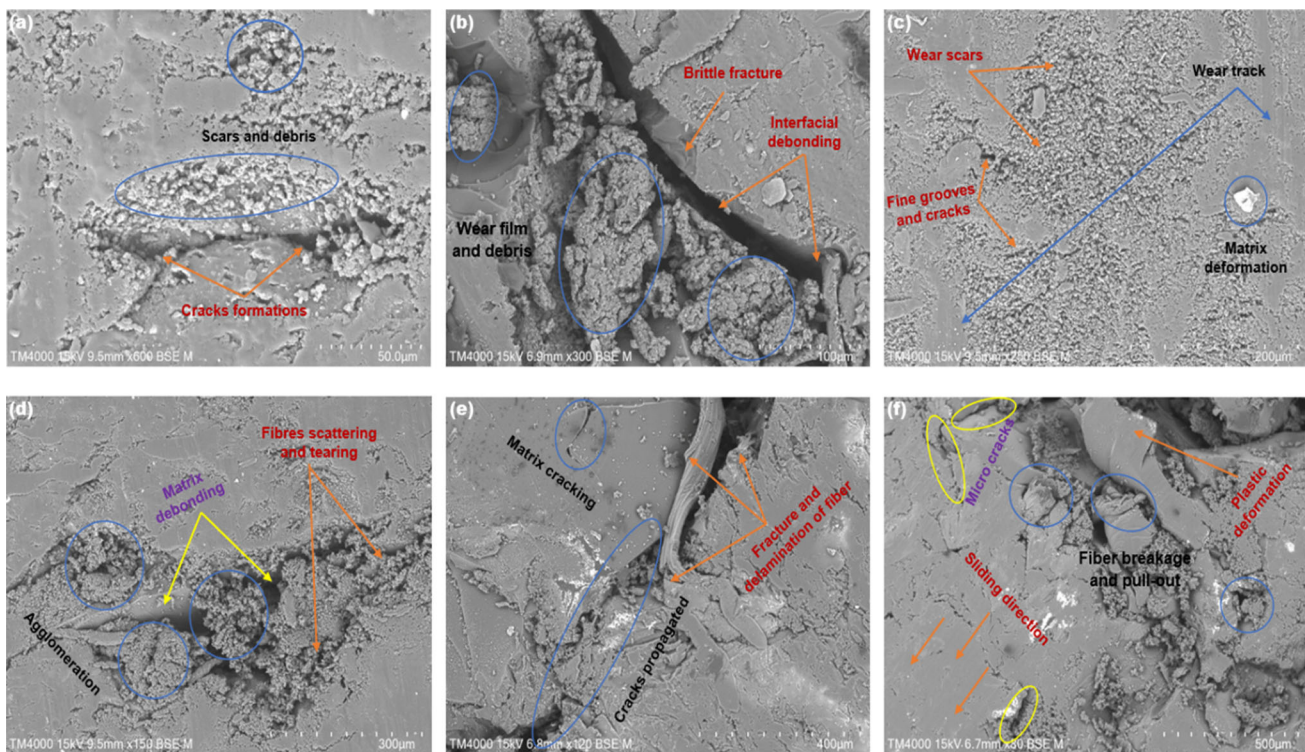


Fig. 11 Surface morphological analysis at worn surface of fabricated green composites

analyzed at higher load then, propagated with increase in sliding distance as shown in Fig. 11e. The increments in

sliding speeds, increased the friction and penetration rate at counter disc thus, matrix materials are plastically deformed

and revealed interfacial debonding between fibers and matrix. Figure 11f analyzed that the micro cracks deformed at higher sliding distance then propagated with increments in sliding speeds. The debonding between fiber and matrix revealed higher material removal and film formations because fiber bundles are failed in terms of pullout, breakage, tearing, scattering, and delamination. The similar types of observation have been also observed from previous studies [64, 66, 70].

4 Conclusion

The study deals with utilization of naturally derived flax and ramie fibers by reinforcing at 10%, 20%, 30%, and 40% weight fractions with bioepoxy resin and fabricated green composites using compression molding process. Three different types of green composites such as flax composites (F), ramie composites (R), and hybrid composites (H) at each weight fraction have been fabricated and characterized their physical, structural and tribological behaviour. Based on the results and outcomes, the following conclusions have been made and summarized below:

- The inclusion of flax and ramie fibers up to 30% showed superficial interfacial adhesion with greater stress transfer from matrix to fibers. The hybridization of flax–ramie composites reduced the water absorption capabilities due to synergetic effects of dual fiber nature and reduced the overall porosity of developed composites (2.58%). The hybridization also enhanced the surface integrity and degrees of crystallinity of composites due to increase in crystalline structure and diffracting peaks.
- The addition of fibers improved the thermal stability and degradation behaviour of composites. The HRC composite recorded maximum degradation temperature (418 °C) with higher char residue at 600 °C (17.77%) and followed by FRC and RRC composites (403 °C and 384 °C) respectively.
- The R-30 composites showed higher surface hardness (69.355) compared to flax composite (58.025) due to resisting the plastic deformation. The hybridization of these fibers improved the surface hardness (63.916) due to increase in interfacial interaction and stiffness of composites.
- The 30% fiber loading (F-30, R-30, and H-30) composites have showed greater wear and friction resistance among other fiber loading composite due to superficial interfacial bond between fibers and matrix. Moreover, the ramie composites analyzed higher wear and tear behaviour compared to flax composites because of higher brittleness properties.
- With increase in applied load from 25 to 50 N, the rate of increments in wear loss (139–144%), frictional force (132–136%), interface temperature (50–52%), and

co-efficient of friction (47–50%) are observed for all composites due to greater penetration rate and friction between samples and counter disc.

- The increments in sliding distance from 500 to 3000 m, enhanced the wear loss for all developed composites and 40% fiber loading composites recorded maximum increments due to clusterization and debonding of fibers. Whereas, the maximum co-efficient of friction are recorded in between 500 and 1250 m of sliding distance because wear debris and micro particles are staked at counter disc that reduce the overall friction.
- The increments in sliding speeds (1 m/s, 2 m/s, and 3 m/s) increased the overall wear and friction performances of developed composites and recorded maximum at 3 m/s due to increase in fiber scattering and tearing at higher speed. The rate of increments in wear loss are quite high (50–55%) compared to frictional coefficient (18–24%) because, wear debris and fiber dusts are stacked on counter disc after 1500 m sliding distance that reduced the generation of friction during rubbing.
- Incorporating the ANN algorithm into the composite substances for all the different circumstances has yielded the most acceptable outcomes and examining the attributes incorporated during the training function. Moreover, the ANN methodology with Purelin function has been recognized as the most appropriate way for quantifying the tribological characteristics of the generated materials.

Therefore, the study concluded that the inclusion of cellulosic fibers with epoxy matrix increased the strength, stiffness, thermal stability and flexibility of composites that resist wear and friction behaviour at higher load due to higher elastic deformation. Whereas, the neat bio-epoxy samples are not able to resist higher load due to lower stiffness and deformation. Therefore, the developed fiber reinforced composite have greater potential to sustained higher load that can be value added materials for structural and load bearing applications like interior cabin design, turbine blades, joints, brake pads, shoes, tires, various belts and hoses.

Acknowledgements The Authors would be very grateful and express their gratitude towards Machine Element Laboratory, Department of Mechanical Engineering at National Institute of Technology Silchar, Assam for giving the necessary facilities to conduct the research study.

Funding This work did not receive any fund from any organizations/industries.

Declarations

Conflict of interest No potential competing interest has been reported for the research/authorship/publication.



References

- Mohanty, A.K.; Misra, M.; Drzal, L.T.: Sustainable bio-composites from renewable resources: opportunities and challenges in the green materials world. *J. Polym. Environ.* **10**, 19–26 (2002)
- Koronis, G.; Silva, A.; Fontul, M.: Green composites: a review of adequate materials for automotive applications. *Compos. B Eng.* **44**(1), 120–127 (2013)
- Drzal, L.T.; Mohanty, A.K.; Misra, M.: Bio-composite materials as alternatives to petroleum-based composites for automotive applications. *Magnesium* **40**(60), 1–3 (2001)
- Wan, Y.Z.; Huang, Y.; He, F.; Li, Q.Y.; Lian, J.J.: Tribological properties of three-dimensional braided carbon/Kevlar/epoxy hybrid composites under dry and lubricated conditions. *Mater. Sci. Eng. A* **452**, 202–209 (2007)
- Chen, B.; Li, X.; Li, X.; Jia, Y.; Yang, J.; Yang, G.; Li, C.: Friction and wear properties of polyimide-based composites with a multiscale carbon fiber-carbon nanotube hybrid. *Tribol. Lett.* **65**, 1–9 (2017)
- Zhou, X.H.; Sun, Y.S.; Wang, W.S.: Influences of carbon fabric/epoxy composites fabrication process on its friction and wear properties. *J. Mater. Process. Technol.* **209**(9), 4553–4557 (2009)
- Nasir, R.M.; Ghazali, N.M.: Tribological performance of paddy straw reinforced polypropylene (PSRP) and unidirectional glass-pultruded-kenaf (UGPK) composites. *J. Tribol.* **1**, 1–17 (2014)
- Omran, E.; Menezes, P.L.; Rohatgi, P.K.: State of the art on tribological behaviour of polymer matrix composites reinforced with natural fibers in the green materials world. *Eng. Sci. Technol. Int. J.* **19**(2), 717–736 (2016)
- Yin, W.; Liu, Z.; Tian, P.; Tao, D.; Meng, Y.; Han, Z.; Tian, Y.: Tribological properties of wood as a cellular fiber-reinforced composite. *Biotribology* **5**, 67–73 (2016)
- Singh, T.; Tejyan, S.; Patnaik, A.; Singh, V.; Zsoldos, I.; Fekete, G.: Fabrication of waste bagasse fiber-reinforced epoxy composites: study of physical, mechanical, and erosion properties. *Polym. Compos.* **40**(9), 3777–3786 (2019)
- Mahakur, V.K.; Bhowmik, S.; Patowari, P.K.: Machining parametric study on the natural fiber reinforced composites: a review. *Proc. Inst. Mech. Eng. C J. Mech. Eng. Sci.* **236**(11), 6232–6249 (2022)
- Mankai, W.; Brahim, S.B.; Smida, B.B.; Cheikh, R.B.; Chafra, M.: Mechanical behaviour study of a lower limb prosthetic socket made of natural fiber reinforced composite. *J. Eng. Res.* **9**(2), 269–277 (2021)
- Zindani, D.; Kumar, S.; Maity, S.R.; Bhowmik, S.: Mechanical characterization of bio-epoxy green composites derived from sodium bicarbonate treated Punica granatum short fiber agro-waste. *J. Polym. Environ.* **29**, 143–155 (2021)
- Yalcin-Enis, I.: Evaluation of recycled textile wastes with E-glass fabric in bio-based epoxy matrix composites: investigation of the mechanical properties. *J. Mater. Cycles Waste Manag.* **25**(1), 171–180 (2023)
- Rwawiire, S.; Tomkova, B.; Militky, J.; Jabbar, A.; Kale, B.M.: Development of a biocomposite based on green epoxy polymer and natural cellulose fabric (bark cloth) for automotive instrument panel applications. *Compos. B Eng.* **81**, 149–157 (2015)
- Bharath, K.N.; Basavarajappa, S.: Applications of biocomposite materials based on natural fibers from renewable resources: a review. *Sci. Eng. Compos. Mater.* **23**(2), 123–133 (2016)
- Kumar, S.; Saha, A.; Bhowmik, S.: Accelerated weathering effects on mechanical, thermal and viscoelastic properties of kenaf/pineapple biocomposite laminates for load bearing structural applications. *J. Appl. Polym. Sci.* **139**(2), 51465 (2022)
- Jagadeesh, P.; Puttegowda, M.; Mavinkere Rangappa, S.; Siengchin, S.: A review on extraction, chemical treatment, characterization of natural fibers and its composites for potential applications. *Polym. Compos.* **42**(12), 6239–6264 (2021)
- Khalid, M.Y.; Imran, R.; Arif, Z.U.; Akram, N.; Arshad, H.; Al Rashid, A.; Garcia Marquez, F.P.: Developments in chemical treatments, manufacturing techniques and potential applications of natural-fibers-based biodegradable composites. *Coatings* **11**(3), 293 (2021)
- Pan, Y.; Zhong, Z.: The effect of hybridization on moisture absorption and mechanical degradation of natural fiber composites: an analytical approach. *Compos. Sci. Technol.* **110**, 132–137 (2015)
- Gupta, M.K.; Ramesh, M.; Thomas, S.: Effect of hybridization on properties of natural and synthetic fiber-reinforced polymer composites (2001–2020): a review. *Polym. Compos.* **42**(10), 4981–5010 (2021)
- Arulmurugan, M.; Prabu, K.; Rajamurugan, G.; Selvakumar, A.S.: Viscoelastic behaviour of aloe vera/hemp/flax sandwich laminate composite reinforced with BaSO₄: dynamic mechanical analysis. *J. Ind. Text.* **50**(7), 1040–1064 (2021)
- Sepe, R.; Bollino, F.; Boccarusso, L.; Caputo, F.: Influence of chemical treatments on mechanical properties of hemp fiber reinforced composites. *Compos. B Eng.* **133**, 210–217 (2018)
- Kumar, S.; Zindani, D.; Bhowmik, S.: Investigation of mechanical and viscoelastic properties of flax-and ramie-reinforced green composites for orthopedic implants. *J. Mater. Eng. Perform.* **29**, 3161–3171 (2020)
- Chares Subash, M.; Muthiah, P.: Eco-friendly degumming of natural fibers for textile applications: a comprehensive review. *Clean Eng. Technol.* **5**, 100304 (2021)
- Fu, Z.; Suo, B.; Yun, R.; Lu, Y.; Wang, H.; Qi, S.; Matejka, V.: Development of eco-friendly brake friction composites containing flax fibers. *J. Reinf. Plast. Compos.* **31**(10), 681–689 (2012)
- QuberK Jeeva Singh, C.; Krishnasamy, P.; Sutrave, S.; Jain, A.: A review on wire mesh reinforced polymer composite. *Polym. Plast. Technol. Mater.* **62**, 1–10 (2023)
- Kamaraj, M.; Manimaran, R.; Datta, S.: Optimization of dry sliding wear parameters of graphene-filled flax fiber-reinforced epoxy composites using Taguchi grey relational analysis. *J. Inst. Eng. (India) Ser. D* **103**, 1–10 (2022)
- Singh, T.; Singh, V.; Ranakoti, L.; Kumar, S.: Optimization on tribological properties of natural fiber reinforced brake friction composite materials: effect of objective and subjective weighting methods. *Polym. Test.* **117**, 107873 (2023)
- Fidan, S.; Oktay, H.; Polat, S.; Ozturk, S.: An artificial neural network model to predict the thermal properties of concrete using different neurons and activation functions. *Adv. Mater. Sci. Eng.* **2019**, 1–13 (2019)
- Ighalo, J.O.; Igwegbe, C.A.; Adeniyi, A.G.; Abdulkareem, S.A.: Artificial neural network modeling of the water absorption behaviour of plantain peel and bamboo fibers reinforced polystyrene composites. *J. Macromol. Sci. Part B* **60**(7), 472–484 (2021)
- Mahakur, V.K.; Paul, R.; Bhowmik, S.; Patowari, P.K.: Influence of surface modification on mechanical and tribology performance of jute filler polymer composites and prediction of the performance using artificial neural network. *Polym. Bull.* 1–22 (2022)
- Kumar, S.; Bhowmik, S.; Zindani, D.: Effect of stacking sequence and thickness variation on the thermo-mechanical properties of flax-kenaf laminated biocomposites and prediction of the optimal configuration using a decision-making framework. *Int. Polym. Proc.* **38**(3), 4341–4355 (2023)
- Nam, S.; Netravali, A.N.: Green composites. I. Physical properties of ramie fibers for environment-friendly green composites. *Fibers Polym.* **7**(4), 372–379 (2006)



35. Ramesh, M.: Flax (*Linum usitatissimum* L.) fibre reinforced polymer composite materials: a review on preparation, properties and prospects. *Prog. Mater. Sci.* **102**, 109–166 (2019)
36. Kumar, S.; Bhowmik, S.; Mahakur, V.K.: Thermo-mechanical and degradation properties of naturally derived biocomposites for prosthesis applications: analysis of the interface pressure and stress distribution on the developed socket. *Proc. Inst. Mech. Eng. Part E J. Process Mech. Eng.* 09544089221131155 (2022)
37. Mahakur, V.K.; Bhowmik, S.; Patowari, P.K.; Kumar, S.: Effect of alkaline treatment on physical, mechanical, and thermal characteristics of jute filler reinforced epoxy composites. *J. Vinyl Add. Tech.* **29**(2), 330–342 (2023)
38. ASTM D 792-98: Standard Test Method for Specific Gravity and Density of Plastic by Displacement. American Society for Testing and Methods, Philadelphia (1998)
39. ASTM Standard D 2734-70: Standard Test Method for Void Content of Reinforced Plastics. American Society for Testing and Materials, Philadelphia (1985)
40. ASTM D785-08: Standard Test Method for Rockwell Hardness of Plastics and Electrical Insulating Materials. ASTM International, West Conshohocken (2002)
41. ASTM - American Society for Testing and Materials. ASTM G99-17. (2017): Standard Test Method for Wear Testing with a Pin-on-Disk Apparatus. Pennsylvania (2017).
42. Prajapati, D.K.; Tiwari, M.: Use of artificial neural network (ANN) to determining surface parameters, friction and wear during pin-on-disc tribotesting. In: *Key Engineering Materials*, vol. 739. Trans Tech Publications Ltd., pp. 87–95 (2017)
43. Mahakur, V.K.; Bhowmik, S.; Patowari, P.K.: Tribo-informatics evaluation of dry sliding friction of silanized jute filler reinforced epoxy composites using machine learning techniques. *Tribol. Int.* **183**, 108388 (2023)
44. Pradhan, P.; Satapathy, A.: Analysis of dry sliding wear behaviour of polyester filled with walnut shell powder using response surface method and neural networks. *J. Mater. Eng. Perform.* **30**(6), 4012–4029 (2021)
45. Fan, X.; Liu, Z.W.; Lu, J.; Liu, Z.T.: Cellulose triacetate optical film preparation from ramie fiber. *Ind. Eng. Chem. Res.* **48**(13), 6212–6215 (2009)
46. Karoyo, A.H.; Dehabadi, L.; Alabi, W.; Simonson, C.J.; Wilson, L.D.: Hydration and sorption properties of raw and milled flax fibers. *ACS Omega* **5**(11), 6113–6121 (2020)
47. Yuan, J.M.; Feng, Y.R.; He, L.P.: Effect of thermal treatment on properties of ramie fibers. *Polym. Degrad. Stab.* **133**, 303–311 (2016)
48. Makhlof, A.; Belaadi, A.; Amroune, S.; Bourchak, M.; Satha, H.: Elaboration and characterization of flax fiber reinforced high density polyethylene biocomposite: effect of the heating rate on thermo-mechanical properties. *J. Nat. Fibers* **19**(10), 3928–3941 (2022)
49. Razali, N.; Sultan, M.T.H.; Jawaid, M.; Md Shah, A.U.; Safri, S.N.A.: Mechanical properties of flax/kenaf hybrid composites. In: *Structural Health Monitoring System for Synthetic, Hybrid and Natural Fiber Composites*, pp. 177–194 (2021)
50. Saha, A.; Kumar, S.; Zindani, D.; Bhowmik, S.: Micro-mechanical analysis of the pineapple-reinforced polymeric composite by the inclusion of pineapple leaf particulates. *Proc. Inst. Mech. Eng. Part L J. Mater. Des. Appl.* **235**(5), 1112–1127 (2021)
51. Ismail, A.S.; Jawaid, M.; Naveen, J.: Void content, tensile, vibration and acoustic properties of kenaf/bamboo fiber reinforced epoxy hybrid composites. *Materials* **12**(13), 2094 (2019)
52. Sanjay, M.R.; Yogesha, B.: Studies on hybridization effect of jute/kenaf/E-glass woven fabric epoxy composites for potential applications: effect of laminate stacking sequences. *J. Ind. Text.* **47**(7), 1830–1848 (2018)
53. Rangaraj, R.; Sathish, S.; Mansadevi, T.L.D.; Supriya, R.; Surakasi, R.; Aravindh, M.; Karthick, A.; Mohanavel, V.; Ravichandran, M.; Muhibbullah, M.; Osman, S.M.: Investigation of weight fraction and alkaline treatment on *Catechu linnaeus/Hibiscus cannabinus/Sansevieria ehrenbergii* plant fibers-reinforced epoxy hybrid composites. *Adv. Mater. Sci. Eng.* **2022**, 1–9 (2022)
54. Sahu, P.; Gupta, M.K.: Eco-friendly treatment and coating for improving the performance of sisal composites. *Polym. Test.* **93**, 106923 (2021)
55. Zindani, D.; Kumar, S.; Maity, S.R.; Bhowmik, S.: Punica granatum fibers as potential reinforcement of composite structures. *Fibers Polym.* **21**, 1535–1549 (2020)
56. Biswal, S.; Satapathy, A.: Preparation, properties and wear performance evaluation of epoxy-palmyra fiber composites. *Polym. Compos.* **39**(6), 1827–1834 (2018)
57. Pradhan, S.; Acharya, S.K.; Prakash, V.: Mechanical, morphological, and tribological behaviour of *Eulaliopsis binata* fiber epoxy composites. *J. Appl. Polym. Sci.* **138**(12), 50077 (2021)
58. Egala, R.; Jagadeesh, G.V.; Setti, S.G.: Experimental investigation and prediction of tribological behaviour of unidirectional short castor oil fiber reinforced epoxy composites. *Friction* **9**, 250–272 (2021)
59. Mysamy, K.; Rajendran, I.: Influence of fibre length on the wear behaviour of chopped agave americana fibre reinforced epoxy composites. *Tribol. Lett.* **44**, 75–80 (2011)
60. Kanakannavar, S.; Pitchaimani, J.; Ramesh, M.R.: Tribological behaviour of natural fibre 3D braided woven fabric reinforced PLA composites. *Proc. Inst. Mech. Eng. Part J J. Eng. Tribol.* **235**(7), 1353–1364 (2021)
61. Yallew, T.B.; Kumar, P.; Singh, I.: Sliding wear properties of jute fabric reinforced polypropylene composites. *Procedia Eng.* **97**, 402–411 (2014)
62. Shuhimi, F.F.; Abdollah, M.F.B.; Kalam, M.A.; Hassan, M.; Amiruddin, H.: Tribological characteristics comparison for oil palm fibre/epoxy and kenaf fibre/epoxy composites under dry sliding conditions. *Tribol. Int.* **101**, 247–254 (2016)
63. Rajeshkumar, G.: A new study on tribological performance of phoenix Sp. fiber-reinforced epoxy composites. *J. Nat. Fibers* **18**(12), 2208–2219 (2021)
64. Correa, C.E.; Betancourt, S.; Vázquez, A.; Gañan, P.: Wear resistance and friction behaviour of thermoset matrix reinforced with Musaceae fiber bundles. *Tribol. Int.* **87**, 57–64 (2015)
65. Kumar, S.; Saha, A.: Effects of particle size on structural, physical, mechanical and tribology behaviour of agricultural waste (corn-cob micro/nano-filler) based epoxy biocomposites. *J. Mater. Cycles Waste Manag.* **24**(6), 2527–2544 (2022)
66. Rashid, B.; Leman, Z.; Jawaid, M.; Ghazali, M.J.; Ishak, M.R.; Abdelgnei, M.A.: Dry sliding wear behaviour of untreated and treated sugar palm fiber filled phenolic composites using factorial technique. *Wear* **380**, 26–35 (2017)
67. Mu, L.; Feng, X.; Zhu, J.; Wang, H.; Sun, Q.; Shi, Y.; Lu, X.: Comparative study of tribological properties of different fibers reinforced PTFE/PEEK composites at elevated temperatures. *Tribol. Trans.* **53**(2), 189–194 (2010)
68. Teli, G.; Mahakur, V.K.; Paul, R.; Bhowmik, S.: Investigation of dry sliding tribological behaviour of epoxy composites filled with hemp particulates using artificial neural networks. *Arab. J. Sci. Eng.* **48**, 1–13 (2022)

69. Mohanty, J.R.; Das, S.N.; Das, H.C.: Tribological behaviour of acrylic acid–modified date palm leaf–reinforced polyvinyl alcohol composite. *Tribol. Trans.* **57**(3), 546–552 (2014)
 70. Singh, N.; Yousif, B.F.; Rilling, D.: Tribological characteristics of sustainable fiber-reinforced thermoplastic composites under wet adhesive wear. *Tribol. Trans.* **54**(5), 736–748 (2011)
- Springer Nature or its licensor (e.g. a society or other partner) holds exclusive rights to this article under a publishing agreement with the author(s) or other rightsholder(s); author self-archiving of the accepted manuscript version of this article is solely governed by the terms of such publishing agreement and applicable law.